Inhibition of LINE-1 retrotransposon-encoded reverse transcriptase modulates the expression of cell differentiation genes in breast cancer cells

Radhika Patnala · Sung-Hun Lee · Jane E. Dahlstrom · Stephen Ohms · Long Chen · S. Thameem Dheen · Danny Rangasamy

Abstract Long Interspersed Elements (L1 elements) are biologically active retrotransposons that are capable of autonomous replication using their own reverse transcriptase (RT) enzyme. Expression of the normally repressed RT has been implicated in cancer cell growth. However, at present, little is known about the expression of L1-encoded RT activity or the molecular changes that are associated with RT activity in the development of breast cancer. Here, we report that RT activity is widespread in breast cancer cells. The expression of RT protein decreased markedly in breast cancer cells after treatment with the antiretroviral drug, efavirenz. While the majority of cells showed a significant reduction in proliferation, inhibition of RT was also accompanied by cell-specific differences in morphology. MCF7 cells displayed elongated microtubule extensions that adhered tightly to their substrate, while a large fraction of the T47D cells that we studied formed long filopodia projections. These morphological changes were reversible upon cessation of RT inhibition, confirming their dependence on RT activity. We also carried out gene expression profiling with microarrays and determined the genes that were differentially expressed during the process of cellular differentiation. Genes involved in proliferation, cell migration, and invasive activity were repressed in RT-inhibited cells. Concomitantly, genes involved in cell projection, formation of vacuolar membranes, and cell-to-cell junctions were significantly upregulated in RT-inhibited cells. qRT-PCR examination of the mRNA expression of these genes in additional cell lines yielded close correlation between their differential expression and the degree of cellular differentiation. Our study demonstrates that the inhibition of L1-encoded RT can reduce the rate of proliferation and promote differentiation of breast cancer cells. Together, these results provide a direct functional link between the expression of L1 retrotransposons and the development of breast cancer.

Keywords Breast cancer cells · Efavirenz · Retrotransposons · LINE-1 · Cell growth · Differentiation · Gene expression

R. Patnala · S.-H. Lee · J. E. Dahlstrom · S. Ohms · L. Chen · D. Rangasamy (✉)
John Curtin School of Medical Research, The Australian National University, Canberra, ACT 2601, Australia
e-mail: danny.rangasamy@anu.edu.au

R. Patnala · S. T. Dheen
Department of Anatomy, Yong Loo Lin School of Medicine, National University of Singapore, Singapore 117597, Singapore

S.-H. Lee
Department of Molecular and Cellular Oncology, The University of Texas MD Anderson Cancer Center, Houston, TX 77030, USA

J. E. Dahlstrom
Department of Anatomical Pathology, The Canberra Hospital, Garran, ACT 2605, Australia

Introduction

Retrotransposons are mobile genetic elements that replicate through an RNA intermediate, which is subsequently copied into genomic DNA by a reverse transcriptase enzyme. At least 45 % of the human genome is derived from repetitive elements formed from retrotransposons. Depending upon whether they contain long terminal repeats (LTRs), retrotransposons are classified into LTR elements (human endogenous retroviruses, HERVs), non-LTR elements (long interspersed elements, LINE-1 or L1 elements), and short interspersed elements (SVA and Alu

elements). L1 elements are the most prolific type of retrotransposon and are capable of mediating insertional mutations, and genome reorganization through their reverse transcriptase enzyme leading to a number of human diseases (reviewed in [1, 2]). There are approximately 7,000 copies of full-length L1 elements in the human genome, at least 100 of which are classified as highly active or retrotransposition-competent [3, 4]. An active L1 element is composed of a 5′-untranslated region, which contains an internal promoter, two open reading frames (ORF1 and ORF2), and a 3′ poly-A tail. ORF1 encodes an RNA-binding protein, whereas ORF2 encodes the reverse transcriptase (RT) and endonuclease enzymes, which are required for the reverse transcription of an L1 RNA intermediate into DNA and the insertion of DNA copies into new genomic locations using a 'copy-and-paste' mechanism [2]. In addition, L1-encoded RT also facilitates the retrotransposition of Alu elements, certain mRNAs and noncoding RNAs to new sites in the host genome [5, 6], thereby reshaping the genome in additional ways. Similar to the L1 element, the HERV element is an autonomous LTR element that can integrate a reverse-transcribed DNA copy of its sequence into the genome using its endogenous RT activity [7]. Since all classes of retrotransposons, except for Alu and SVA elements, contain an RT-encoding gene, the activity of RT has been implicated in a range of retrotransposon-mediated human diseases [8, 9]. Furthermore, the presence of RT itself, has been associated with several cellular and physiological disorders [10].

The majority of human cancer cells, cancer-derived cell lines and a variety of transformed cells have a high level of L1 expression, but L1 elements are rarely expressed in noncancerous cells or morphologically differentiated somatic tissues [11–13]. It has also been shown that the breast carcinoma-derived T47D cell line releases retroviral-like particles that possess a high level of RT activity [14]. The level of RT is also particularly high in patients with lymphoma and breast cancer, but drops dramatically after cancer treatment [15, 16], suggesting a potential link between RT activity and the proliferative potential of cancer cells. Several studies have shown that antiretroviral non-nucleoside reverse transcriptase inhibitors (NNRTIs) such as efavirenz and nevirapine bind to a hydrophobic region of the RT enzyme, inducing a conformational change in the enzyme and consequently inhibiting RT activity [17]. Efavirenz is a first-line antiretroviral drug, and is widely used to treat HIV-1 infections. Recently, Efavirenz has been reported to suppress the activity of the L1-encoded RT enzyme, similar to the effect of small interference RNA against L1 elements, and to promote morphological differentiation in melanoma A-375 cells [18, 19]. Consistently, other NNRTI drugs have been found to inhibit L1 retrotransposition activity in a number of human cells [20–22]. More recently, another class of RT inhibitors, the nucleoside reverse transcriptase inhibitors (NRTIs) have also been shown to suppress L1 activity and to induce anticancer activity in prostate cancer cell lines [23], suggesting that inhibition of the L1-encoded RT might be a potential target for diagnostic and therapeutic intervention. Despite these findings, many questions remain unclear about the molecular changes, and the extent of changes in gene expression that result from RT inhibition. Moreover, little is known about how inhibition of RT can lead to morphological changes in cancer cells.

Breast cancer is the most common malignant diseases with an increasing worldwide incidence and is a leading cause of death in women. There is an urgent need to diagnose and treat breast cancer in its early stages. We recently discovered that L1 elements are differentially expressed between normal and breast tumor tissues. L1 is barely expressed, if at all, in normal healthy cells, while in contrast, it is overexpressed in almost all breast cancer cells and clinical samples [24, 25]. However, little is known about the role of L1 elements or L1-encoded RT activity in the process of breast cancer development. Given that NNRTIs can inhibit RT activity, we investigated the anticancer effects of efavirenz on various breast cancer cell lines. Here, we report that inhibition of RT promotes growth arrest, differentiation, and morphological changes in cancer cells. We also demonstrate that efavirenz activates differentiation-specific gene expression signatures and reprograms the activation of many genes that can restore control of the growth and differentiation processes of breast cancer cells.

Materials and methods

Cell cultures and drug treatments

Normal human breast epithelial cells (HMECs) and mammary epithelial growth medium (MEGM Bullet Kit) were obtained from Lonza (Walkersville, MD). The HMEC (Lonza-CC-2551) and non-tumorigenic MCF10A cells (ATCC-CRL-10371) were cultured in the MEGM Bullet Kit (Clonetics) supplemented with 10 µg/ml of insulin. MCF7, T47D, SKBR3, Hs578T, BT20, HBL100, and MDA-MB-231 cell lines were obtained from ATCC and cultured in Dulbecco's modified Eagle's medium (DMEM) with 2 mM L-glutamine and 10 % FCS at 37° C in 5 % CO_2. MDA-MB-361 cells were cultured in Leibovitz's L-15 Media (Invitrogen) with 20 % FBS. Efavirenz was obtained from the NIH AIDS Research and Reference Reagent Program. Efavirenz was dissolved in dimethyl sulfoxide (DMSO) at a final concentration of 0.2 % and used at concentrations of 15 and 45 µM as described

previously [18]. The same volume of DMSO was added to controls. Cells were treated with or without drug 24 h after seeding into 6-well plates at a density of 2×10^4 cells/well. Medium was replaced with fresh efavirenz or DMSO every 24 h. Cells were harvested after 72 h of treatment. To assess the effect of drug withdrawal, cells were treated with drug for 72 h, then washed twice with PBS and cultured in fresh medium for 48 h without drug or DMSO.

Western blot analysis

Cell lysates were prepared using MPER reagent (Pierce). Protein samples were separated on a 4–12 % Bis–Tris polyacrylamide gel (Invitrogen) and transferred onto Nylon membranes (GE Healthcare). Western blot analysis was performed with anti-L1 ORF2p antibodies at 1:3000 dilution [25], followed by addition of HRP-conjugated secondary antibodies (Dako Cytomation). The resulting signals were visualized using the ECL chemiluminescence system (Pierce) and quantified by densitometry using NIH ImageJ software. To confirm protein normalization, the membranes were stripped and reprobed with α-tubulin antibodies (Sigma).

Reverse transcriptase assay

Whole-cell lysates were prepared as described previously [23]. RT assays were carried out in 20-µl reactions containing 10 ng of MS2 phage RNA (Roche) and RT-PCR reaction buffer (Invitrogen), 0.5 mM of dNTP mix, 2U of RNAseOUT, 50 pmol of MS2 reverse primer, and 20 µg of whole-cell lysates. The reaction mixture was incubated at 55 °C for 60 min, followed by addition of 2U of RNaseH (Invitrogen) and incubated further at 37 °C for 20 min. Control reactions were set up by either omitting cell lysates or adding 1 µl of commercially available RT enzyme (Invitrogen). About 2 µl of the resulting reaction was subsequently amplified using the MS2 primers: forward 5′-CCTGCTCAACTTCCTGTCGAG-3′, reverse 5′-CATAG GTCAAACCTCCTAGGAAT-3′. PCR was carried out at standard amplification parameters (95 °C for 10 min, followed by 30 cycles of 95 °C for 15 s, 55 °C for 30 s and 72 °C for 45 s and final extension at 72 °C for 5 min). The PCR products were analyzed by electrophoresis using a 2 % agarose gel.

Quantitative RT-PCR analysis

Total RNA was isolated from cells using an RNeasy Kit (Qiagen) and digested with TurboDNase-I (Ambion). About 2 µg of purified RNA was used for cDNA synthesis with 0.1 µg random decamer primers using a RETRO-Script RT kit (Ambion). The resulting cDNAs were used as templates for real-time qRT-PCR with specific primers for L1 ORF1 and ORF2 and a selection of genes found to be differentially expressed genes including CDC42, EXOC4, PARD3, PTPA4, and HPRT1: L1 ORF1 forward 5′-GGTT ACCCTCAAAGGAAGCC-3′, reverse 5′-GCCTGGTGAC AAAATCTC-3′; L1 ORF2 forward 5′-AAATGGTGCTGG GAAAACTG-3′, reverse 5′-GCCATTGCTTTTGGTGTTTT -3′; CDC42 forward 5′-CATCTCTCCAGAGCCCTTTC-3′, reverse 5′-TGCAGGGCATTTGTCATTAT-3′; EXOC4 forward 5′-CTGGACTTTGCAAGGCAGTA-3′, reverse, 5′-CT CCAGCTCCGTGTACTTCA-3′; PARD3 forward 5′-TTGA TGAGCAGGATCCACAT-3′, reverse, 5′-AGGCTGAAAG GCTGAGACAT-3′; PTPA4 forward 5′-ATGAGAAACGTG GTTTGCAG-3′, reverse, 5′-GATGCAGGAAGCCTGAAGT T-3′; HPRT1 forward 5′-CCTGGCGTCGTGATTAGTGAT-3′, reverse 5′-AGACGTTCAGTCCTGTCCATA-3′. As a negative control, we synthesized cDNA in the absence of reverse transcriptase and primers. Real-time qRT-PCR was carried out with SYBR Green PCR master mix and a 7900HT thermal cycler (Applied Biosystem) with typical amplification parameters (50 °C for 2 min and 95 °C for 10 min, followed by 40 cycles of 95 °C for 15 s and 60 °C for 1 min). Fold changes were determined by comparing the ΔC_T value of each gene normalized to the reference control HPRT1 for each reaction. Data generated were the average of three independent experiments, with each experiment performed in triplicate and analyzed using the Relative Expression Software Tool (http://REST.gene-quantification.info).

Cell proliferation and cell cycle analysis

Cells were seeded in 96-well plates at a density of 1×10^3 cells/well in 100 µl of culture medium with or without drug for 72 h. Proliferation of cells in response to drug were determined with an ELISA reader after staining with XTT (2,3-Bis-(2-methoxy-4-nitro-5-sulfophenyl)-2H-tetrazolium-5-carboxanilide) at various time points, as described by the manufacturer (Applichem). Assessment of apoptosis was carried out using combined staining with PI and FITC-labelled Annexin V (BD Biosciences), following the manufacturer's instructions. The cell-cycle phase distribution was determined by flow cytometry. In brief, cells were stained with 7AAD (7-amino-actinomycin D), and incubated with Anti-Human Ki-67 Alexa Fluor647 antibody (eBiosciences) at 1:150 dilutions for 30 min at 4 °C. Cells were then analyzed using a LSRFortessa cell analyzer (BD Biosciences), and data analyzed using FlowJo version 7.6.4 software.

Immunofluorescence analysis

Cells were grown on glass coverslips in 12-well plates at a density of 1×10^3 cells per well. Cells were fixed in 4 %

paraformaldehyde for 10 min and permeabilized in 0.25 % Triton X-100 for 15 min. Mouse monoclonal anti-tubulin antibody (Sigma) was visualized by staining with FITC-conjugated secondary antibody (Jackson ImmunoResearch). Nuclei were stained with 0.1 μg/ml DAPI. Images were overlaid in Adope Photoshop.

Scanning electron microscopy

Cells were fixed in 2 % glutaraldehyde in 0.1 M sodium cacodylate buffer, pH 7.4 at 4 °C overnight, followed by secondary fixation with 1 % osmium teroxide for 90 min and then dehydrated with increasing concentrations of acetone. Sample's critical-point drying was performed with liquid CO_2 using Balzers CPD-020, Liechtenstein, followed by gold coating with a Polaron gold coater. Images were taken with a Hitachi S-4300SE/N electron microscope at 3 kV, aperture no. 3 and 9.7 mm.

Microarray analysis

Total RNA was isolated from cells using an RNeasy Kit (Qiagen) and the RNA integrity evaluated with an Agilent 2100 Bioanalyzer. Approximately 20-μg RNA was labeled with Cy3-conjugated dCTP (Amersham) using the PrimeScript (Takara) reverse transcriptase. Labeled cDNA was hybridized for 16 h at 42 °C to Roche NimbleGen Human Whole Genome 12-plex arrays according to the manufacturer's protocol. The arrays were analyzed with an Axon GenePix 4000B scanner and associated software (Molecular Devices). Gene expression levels were calculated with NimbleScan Version 2.4 (Roche NimbleGen, Inc., WI). Relative signal intensities for each gene were generated using the Robust Multi-Array Average algorithm with quantile normalization and summarized by the median polish method with NimbleScan Version 2.4 (Roche NimbleGen). The log2 gene expression values were then analyzed for fold changes in GeneSpring GX 11 (Agilent Technologies, CA). The criteria for differential gene expression were that gene expression levels be at least 2-fold upregulated or 0.5-fold downregulated compared to control values, combined with a p value ≤ 0.5 after correction for multiple testing with the Benjamini–Hochberg algorithm.

Functional clustering analysis

The DAVID functional annotation tool, from NIH (http://david.abcc.ncifcrf.gov/tools), was used for gene ontology (GO) enrichment analysis, using the DAVID default human population background. Three lists of genes (upregulated or downregulated 2-fold or greater) were uploaded to the DAVID website, which analyses gene lists and clusters genes into groups according to enrichment of annotations compared to a background gene list. The frequency of each GO term keyword in a gene list is compared to that for the entire human genome (termed the "background"), providing a measure of enrichment of a particular annotation in a gene list compared to what would be expected from random chance. An enrichment p value based on a hypergeometric test is calculated together with a p value corrected for multiple testing. The enrichment p values for a cluster of similar annotation terms can be combined and an average value calculated using a geometric mean to give a single enrichment score for a cluster. An enrichment score ≥ 1.3 is regarded as statistically significant by DAVID.

Statistical analysis

The data obtained from all experiments were expressed as the mean ± SD of three independent experiments with each experiment performed in triplicate. A two-tailed unpaired student's t test was used to estimate statistical significance using Prism software (GraphPad Software, San Diego, CA). P (probability) < 0.05 was accepted as statistically significant.

Results

RT activity in breast cancer cells

In a recent study we reported that L1-encoded ORF2p, which contains the reverse transcriptase (RT) enzyme, is significantly overexpressed in breast tumors of various stages and grades [25], but the functional significance of this increase in expression was unclear. To gain insight into the mechanisms by which L1-encoded RT contributes to breast cancer, we first evaluated endogenous RT activity in primary mammary epithelial cells (HMEC or its immortalized cell line counterpart, MCF10A) and a panel of breast cancer cell lines (MCF7, T47D, SKBR3, Hs578T, BT20, MCF-7, MDA-MB-361, MDA-MB-436, and MDA-MB-231). Extracts isolated from these cells were used as sources of RT to reverse transcribe a synthetic MS2 phage RNA. The NTera.2D1 human embryonic carcinoma cell line, which expresses high levels of L1 protein [13], were used as a positive control. As shown in Fig. 1a, RT activity was found in all breast cancer cell lysates tested, indicating that the synthetic MS2 RNA had been successfully reverse-transcribed into a cDNA product at the expected band size of 110 bp. As expected, none of the normal breast MCF10A or HMEC cell lines showed RT activity, suggesting that RT proteins are abundantly present in breast cancer cells but not in non-tumorigenic cell lines.
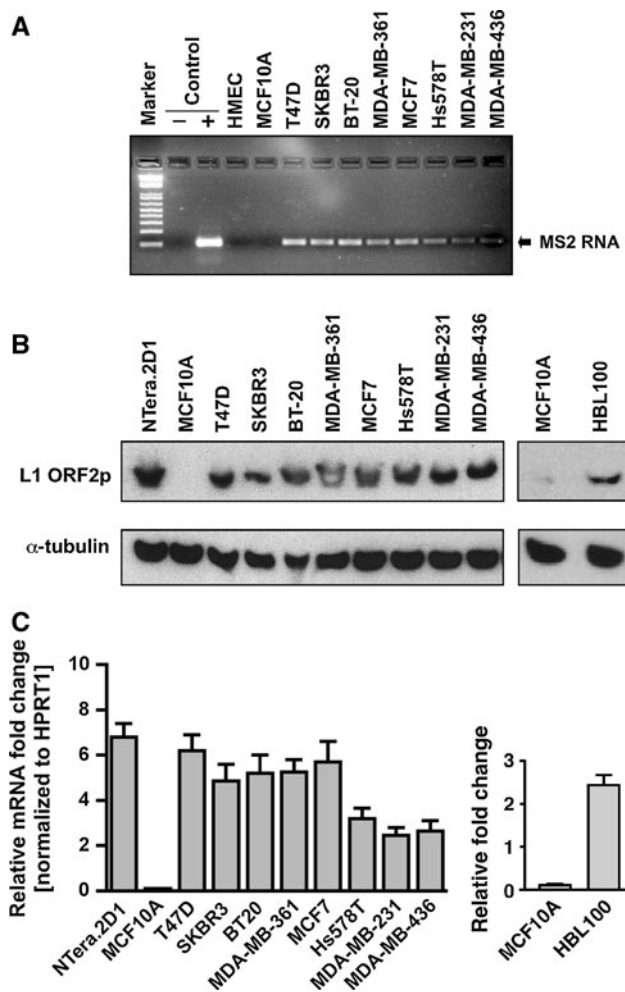
Fig. 1 L1-encoded RT activity in breast cancer cells. a Endogenous RT activity was detected after incubation of synthetic MS2 phage RNA with cell extracts from a panel of breast cancer cells. Control reactions were set up by omitting cell extract (negative control) or adding cell extracts from NTera.2D1 human embryonic carcinoma cells (positive control). The PCR product of 110 bp (corresponding to the reverse-transcribed MS2 cDNA) is shown. Marker, 1 kb-plus DNA marker. b The L1-encoded ORF2p, which contains the RT enzyme, was detected by western blotting of whole-cell lysates from normal and a panel of breast cancer cells. NTera.2D1 were used as positive controls. For protein normalization, α-tubulin was used as a loading control. c The L1 ORF2 mRNAs derived from L1 expression were quantified by qRT-PCR with primer specific for the ORF2 sequence. The data are shown as fold change in each breast cancer panel cells compared to normal MCF10A after normalization to the HPRT1 housekeeping gene. Each point represents the average of three independent experiments, with each experiment performed in triplicate. Error bars indicate SD ($n = 3$)

To further assess the expression profile of RT across this panel, cell lysates were subjected to western blot analysis for L1 RT expression using anti-L1 ORF2p antibodies [25]. Despite the assay not being quantitative, this analysis revealed that all breast cancer cells express L1 ORF2p at the expected size of ~150 kDa (Fig. 1b). The MCF10A normal breast cell line showed no expression except for occasional background staining. Furthermore, the relative expression levels of L1 ORF2 mRNA, which is an essential prerequisite of RT, were notably higher in some of the noninvasive and marginally invasive cell lines (T47D, SKBR3, MCF7, and Hs578T) compared to the highly invasive breast cancer cell lines (MDA-MB-231, MDA-MB-436) as measured by qRT-PCR assays (Fig. 1c). This suggests that RT might become activated in the early stages of malignant transformation. The observation of early activation of L1-encoded RT is in agreement with DNA methylation studies in which the early onset of L1 demethylation has been reported to activate L1 expression during cancer progression [26]. Overall, these results suggest that L1-encoded RT activity is widespread in breast cancer cells, and that it could, in principle, serve as a target to inhibit its activity and to understand the function of RT activity in cancer cells.

RT inhibition promotes cellular differentiation

RT inhibitors such as nevirapine and efavirenz are commonly used in antiretroviral therapy for patients infected with HIV-1. Their key role is to inhibit the catalytic activity of the RT p66 subunit, thereby blocking viral DNA synthesis [17, 27]. In humans, the most abundant source of RT activity are L1 retrotransposons, which represent approximately 21 % of the genome, and thus L1-encoded RT is assumed to be one of the targets of RT inhibitors. Recent studies show that efavirenz has a higher affinity to L1-encoded RT than nevirapine [21, 22] and is a more effective inhibitor of RT activity. To analyse the effect of inhibiting L1-encoded RT, we used efavirenz at concentrations of 15 and 45 µM as described previously [18]. The noninvasive breast cancer T47D cells, which possess a high level of RT activity [14], were treated with efavirenz for 72 h or mock-treated DMSO without drug, followed by an assessment of the effect of drug treatment on L1 protein expression. As shown in Fig. 2a, an approximately 70 % decrease in the level of L1-encoded RT protein was observed in T47D cells after efavirenz treatment (71 ± 4 % for 15 µM and 77 ± 9 % for 45 µM of efavirenz compared with mock-treated cells as measured by densitometry using NIH ImageJ software). To further confirm the decrease in expression of L1 RT protein, we measured the relative expression of L1 mRNA using qRT-PCR analysis (Fig. 2b). In this assay MCF10A cells, which do not express L1 mRNA, served as controls. As expected, a two-fold decrease in the levels of ORF2 mRNA ($p < 0.001$, unpaired t test) was observed in both 15 and 45 µM efavirenz-treated cells compared with mock-treated cells. Interestingly, we did not observe significant changes in the expression of L1 ORF1 mRNA ($p > 0.05$), although the relative levels of ORF1 mRNA expression were lower
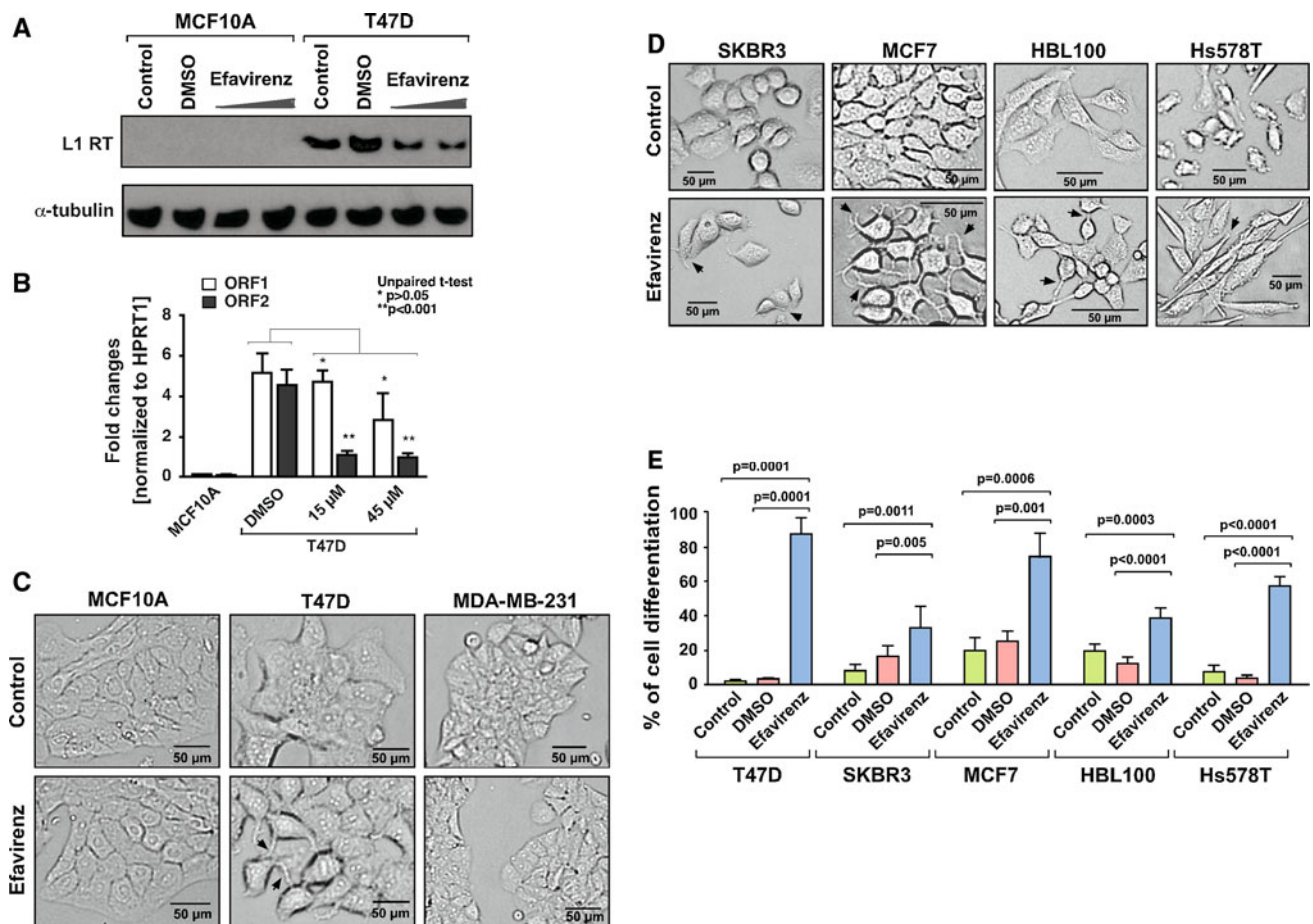
Fig. 2 RT inhibition promotes differentiation in breast cancer cell lines. **a** Western blots of L1-encoded RT protein in normal (MCF10A) and breast cancer (T47D) cells after treatment with 15 and 45 μM efavirenz for 72 h. The analyses of the parental cells (control) and cells treated with DMSO (mock) were performed in parallel. α-tubulin was used as an internal control. **b** Quantitative real-time RT-PCR analysis of endogenous L1 mRNAs in T47D cells that were treated with 15 and 45 μM efavirenz or DMSO for 72 h. The MCF10A cell line was used as a negative control. The data are shown as the relative fold changes of ORF1 and ORF2 mRNAs with respect to the control HPRT1. The error bars indicate SD ($n = 3$). Unpaired t test, * $p > 0.05$ and ** $p < 0.001$. **c** Morphological differentiation of normal MCF10A and breast cancer T47D and MDA-MB-231 cells

after treatment with 15 μM efavirenz or DMSO (control) for 72 h. Representative panels from phase-contrast microscopy are shown. *Bar* 50 μM. **d** Phase-contrast microscopy of weakly-and-moderately-invasive breast cancer cells. Cells exposed to DMSO (control) or efavirenz were examined in vivo after 72 h of culture to assess morphological changes. The *arrows* indicate the appearance of filopodial projections on the cell edges. **e** Quantitative morphological changes. The percentages of morphological changes in drug-treated cells were calculated by comparison to mock DMSO-treated cells or parental cells in 100 cells from ten randomly selected fields. Each point represents an average from two independent experiments. *P* values were calculated by unpaired *t* test in comparisons to mock-treated and parental cells. *Error bars* indicate SD

in cells treated with drug compared with mock-treated cells.

Normal epithelial cells synthesize adhesion proteins and assemble and adhere to extracellular basement membranes such as laminin and fibronectin and a loss of the ability to interact with the basement membrane is one of the features of the neoplastic proliferation of epithelial-derived cancer cells [28, 29]. In fact, the phenotypic changes associated with extracellular matrix interactions are often used as criteria to establish the degree of differentiation in cancer studies and pathological diagnosis [30]. Having confirmed that efavirenz can effectively inhibit L1 RT expression, we

next investigated the phenotypic changes that occur during drug treatment. MCF10A normal breast cells and T47D and MDA-MB-231 breast cancer cells were cultured with 15 μM efavirenz for 72 h. The noninvasive T47D cancer cells showed significant cellular differentiation following efavirenz treatment. A majority of the drug-treated cells exhibited monolayer growth, with distinct cell borders and shapes. In contrast, control cells grew in multilayer clumps with indistinct cell borders (Fig. 2c). Notably, the MCF10A normal breast cell line did not show any changes in cellular differentiation either with, or without drug treatment. This was mainly due to the lack of L1

expression in MCF10A cell line. Interestingly, the highly invasive metastatic MDA-MB-231 cells responded poorly to drug treatment, even after 50 μM efavirenz (a three-fold higher concentration) and 120 h of exposure (data not shown). These observations suggest that efavirenz selectively controls the differentiation of some, but not all, breast cancer cells.

To further confirm if the response to drug treatment varied between the different cell types in the panel, we assessed the effect of efavirenz on the differentiation of several other noninvasive and marginally invasive breast cancer cells (SKBR3, MCF7, HBL100, and Hs578T). We found that cellular differentiation, as denoted by cell shape, a decreased tendency to form aggregates, and increased cell adhesion, became apparent after exposure to drug compared to control cells (Fig. 2d). This development of a differentiated morphology is in agreement with previous study where similar changes in morphology were noticed in nevirapine-treated breast carcinoma cell lines [31]. Using phase-contrast microscopy ($n = 100$ cells from ten randomly selected fields), we quantified the percentage of differentiation based on morphological changes such as changes in cell shapes and cell adhesion, or the presence of distinct cell borders. In parallel we also evaluated whether these morphological changes had an effect on the structure of the cytoskeleton using immunofluorescence assays as described in previous reports [18, 31]. These included structural changes in the cytoskeleton, notably the formation of elongated microtubules and monolayer cell growth. T47D cells showed the greatest response, with a 4.5-fold increase in the rate of cell differentiation (Fig. 2e). A similar effect was also seen in MCF7 and Hs578T-treated cells, although it was quantitatively less pronounced, indicating that RT inhibition may play a key role in the differentiation of some of the breast cancer cell lines.

Effects of RT inhibition on filopodia formation

Cellular differentiation is often characterized by the formation of elongated microtubules, with the cells resuming contact inhibition and developing into monolayer cultures [32]. On the other hand, cancer cells lose contact inhibition and proliferate as multilayers with indistinct cell borders. Filopodia and microvilli are believed to play important roles in cell-to-cell contact between layers and in aligning cells when they adhere to extracellular matrix (reviewed in [33, 34]). The formation of filopodia occurs when cells move along certain cell differentiation-related pathways. It has been shown that filopodia formations occurs in cells following induction of CDC42 [35] and that filopodia are the location of many functionally important membrane proteins, which are involved in signal transduction pathways, glucose transport and energy metabolism required

for morphological differentiation [36, 37]. Interestingly, the microtubule cytoskeletons are also required for spatial regulation of filopodia projections [38]. Although the exact functions of filopodia remain unclear, the increased numbers of filopodia structures have been shown to affect cellular morphology by changing the attachment of cells to adjacent surfaces [33].

Since efavirenz induces cellular differentiation, we wondered whether the process of differentiation was due to the formation of filopodia projections. Our observation of cells under phase-contrast microscopy and immunofluorescence assays (using randomly selected fields) revealed clear signs of differentiation in drug-treated cells, with the appearance of cell surface projections and elongated microtubules that adhered tightly to the surface of cell culture dish (see Figs. 2c, d), similar to the filopodia projections seen in melanoma and fibroblast cells [39]. Strikingly, the formation of filopodia varied between the cell types. About 80 % of T47D cells responded to drug by forming filopodia on their edges, connecting to the bodies of neighboring cells. In contrast, only a few control T47D cells formed filopodia. By scanning electron microscopy (SEM), we examined the surface architecture of the cells treated with or without drug (Fig. 3a). Efavirenz-treated T47D displayed numerous filopodial projections, as well as infrequent large blebs on their cell surfaces and the surfaces had a very smooth texture. In contrast, control cells exhibited shortened filopodia with a decrease in the number of filopodia and the cell surface developed a wrinkled texture. In the case of MCF7 cells, although the majority of cells displayed filopodial structures, many efavirenz-treated cells also had elongated microtubule extensions, different from those of control MCF7 cells, in which short microtubules concentrated around nucleating centers. To further confirm the presence of the microtubule extensions, cells were subjected to immunofluorescence staining with anti-tubulin antibody, as a marker of the microtubule cytoskeleton [32]. As shown in Fig. 3b, the drug-treated MCF7 cells displayed elongated microtubules, with the appearance of fusiform extensions protruding from the cell periphery. In contrast, control cells contained few, if any, microtubule extensions, suggesting that the microtubule cytoskeletons were reorganised in response to drug. These observations are consistent with earlier studies where similar changes in microtubules were noticed in nevirapine-treated melanoma cells [18, 31]. Interestingly, T47D cells did not show significant changes in microtubule extensions either with, or without drug treatment. Furthermore, Hs578T cells had no filopodia structures at all. Instead, drug-treated cells become flattened compared to untreated cells and exhibited a distinctive elongated and reorganised clustering morphology, with a resumption of contact inhibition (Fig. 2d and data not shown). Taken
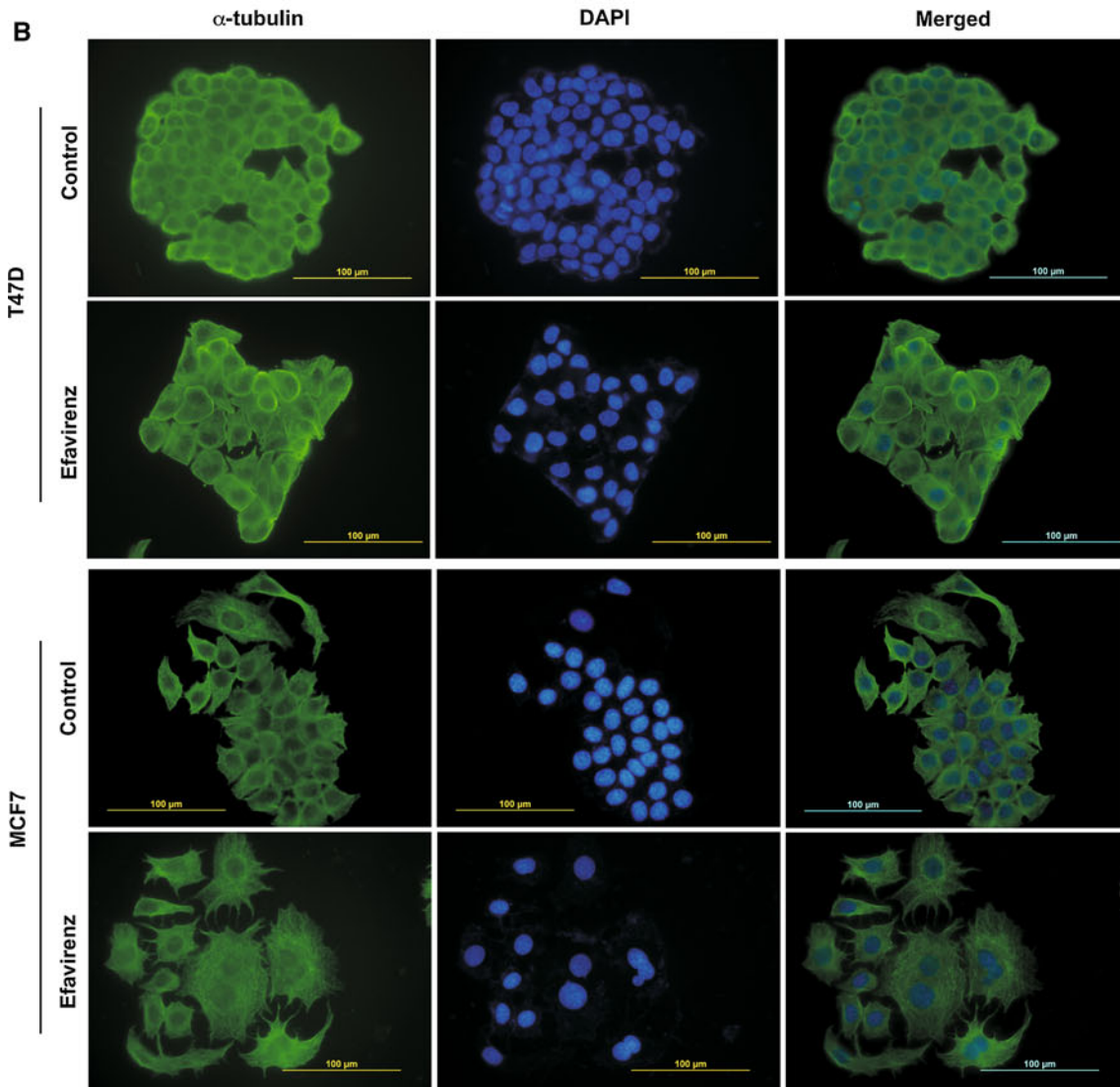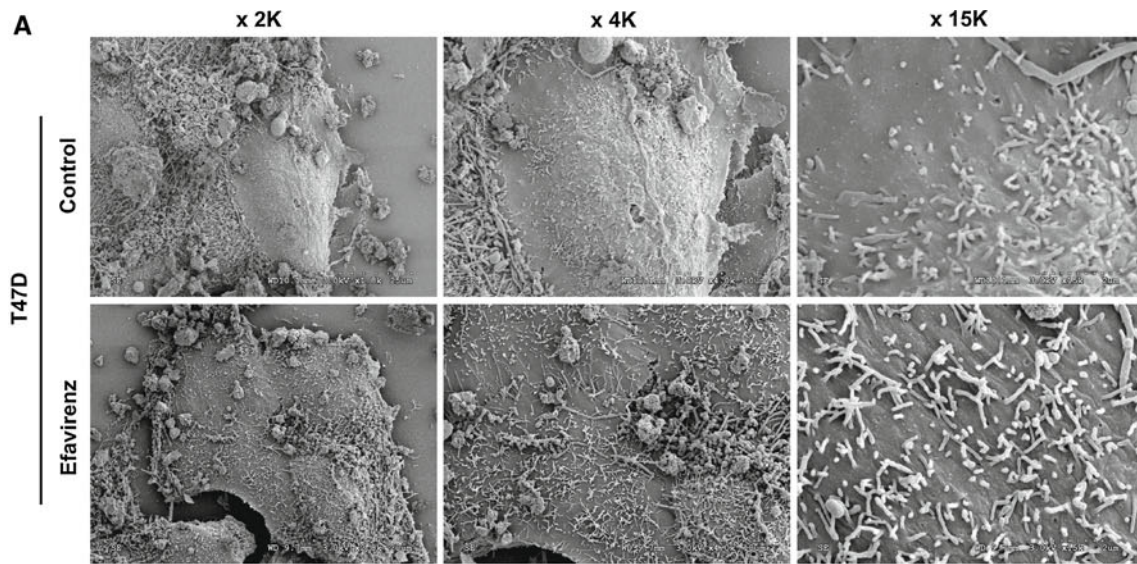
◄**Fig. 3** RT inhibition leads to distinct changes in the surface architecture of cells. **a** Scanning electron microscopy images illustrates the formation of filopedial projections in DMSO-treated control and RT-inhibited T47D cells. **b** Immunofluorescence of T47D and MCF7 cells in the absence (control) or presence of RT inhibition (efavirenz). Cells stained with anti-tubulin (*green*) and DAPI staining of nucleus (*blue*) are shown. *Bar* represents 100 μM

together, these observations suggest that efavirenz induces morphological differentiation in a manner that is dependent upon on the particular cell type.

RT inhibition reduces cell proliferation

To determine whether efavirenz had direct functional effects on the rate of cell growth and proliferation, cells were cultured with or without drug and cell proliferation and viability assessed with XTT assays. We detected a statistically significant decrease in the rate of cell proliferation of drug-treated T47D, MCF7, and Hs578T cells

compared to parental cells or mock-treated controls (Fig. 4a). Some cell type-specific differences were also observed in the response to efavirenz. T47D cells had the most pronounced response with a 60 % decrease in cell proliferation, followed by 44 % in MCF7 cells. Hs578T cells showed a weaker response to the drug, with a 33 % reduction in the cell proliferation rate. To further confirm the inhibitory effect of drug, cells were cultured with efavirenz for 72 h, followed by growth in drug-free media for 48 h (Fig. 4b). The subsequent assays showed that, in the absence of efavirenz, proliferation resumed to a rate almost comparable to that of control cells, suggesting a reversible effect of the drug on cell growth, consistent with previous reports [18, 20]. To investigate whether the decrease in cell proliferation was due to apoptosis of drug-treated cells, cells were stained with a combination of 7-AAD (to detect dead cells) and the proliferation marker Ki-67, and analysed by flow cytometry to identify cycling cells. No significant differences in the induction of cell death were observed in T47D, MCF7, and Hs578T cells with or

Fig. 4 RT inhibition reduces proliferation in breast cancer cells. **a** 1×10^3 cells were seeded in 96-well plates, cultured with or without efavirenz at the concentration of 15 μm for 72 h and color formation measured at absorbance 492 nm after 2, 6, and 20 h incubation with XTT. Analysis of parental cells was performed in parallel. The reference wavelength was measured at the absorbance 690 nm. The staining intensity represents the ratio of absorbance at 492 and 690 nm. *Error bars* indicate SD of three independent assays. **b** An equivalent number of cells were cultured in the presence of efavirenz for 72 h and the cells then counted and replated in drug-free medium for 48 h. Proliferation in response to drug-free medium was measured using an ELISA reader after staining with XTT. The (*) and (**) symbols denote a significant difference compared to drug-treated cells, with a *p* value < 0.05 and <0.001, respectively
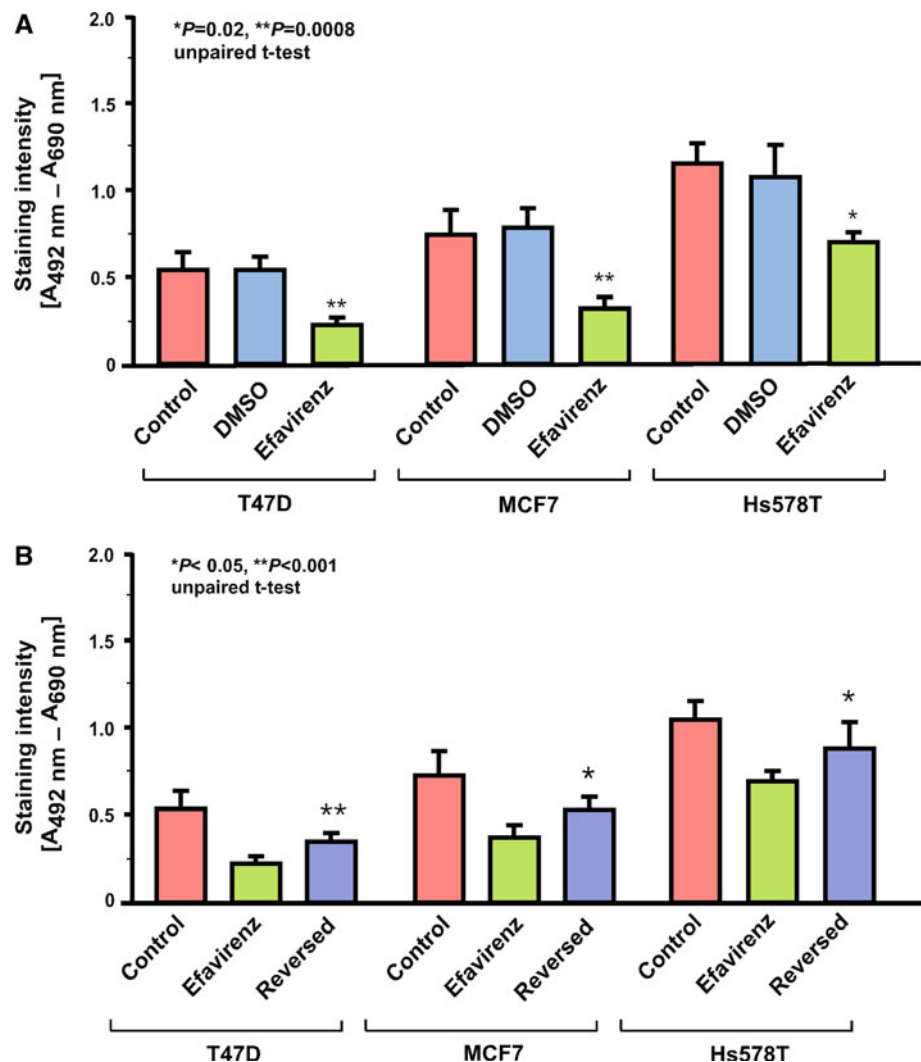
without drug treatment. At most, 17 % of cells were recorded as having undergone apoptosis in both controls and drug-treated cells (data not shown), suggesting that drug had no specific effect on cell death or cytotoxicity.

Distinct gene expression signatures are associated with RT inhibition

Having observed that efavirenz influenced cell growth and morphological differentiation, we set out to investigate differences in gene expression in drug-treated and untreated cells. To accomplish this, we isolated total RNA from DMSO-treated control and drug-treated T47D cells and carried out gene expression analysis using Nimblegen cDNA arrays (Build Hg18; 45,035 genes). We explored the microarray results by carrying out gene ontology enrichment analyses on the lists of 303 upregulated and 352 downregulated genes that were significantly different in response to the drug treatment as determined by a student's t test (p values ≤ 0.05 after correcting for multiple testing using the Benjamini–Hochberg algorithm) and expression fold changes ≥ 2 (upregulated) or ≤ 0.5 (downregulated). The lists of differentially regulated genes were analysed with the DAVID gene ontology web server (Database for Annotation, Visualization, and Integrated Discovery). The most significant gene clusters, with enrichment scores ≥ 1.3 (equivalent to a p value of 0.05 on the non-log scale) are listed in Table 1. The heat map in Fig. 5a shows a consistent pattern of change in the gene that were identified by the DAVID analysis and with false discovery rate (FDR) < 0.05 in the univariate analysis. The first-most significant upregulated gene cluster contained genes involved in cell projection and the formation of dendritic spines (CDC42, FBX02, EXOC4, RSHL3, TTLL9, and ATP1A2). The second-most significant cluster contained genes involving the vacuolar membrane (ARL8A, ATP6V1G2, SBF2, and STX8). Upregulation of cell projection genes that are essential for the biogenesis of cell surfaces and genes in signaling pathways that control the extension and maintenance of filopodia are likely to be responsible for the differences in differentiation and growth observed in these cells. Interestingly, the third most significant gene cluster with a lower enrichment score of 1.17 contained many genes involved in cell junction formation (PARD3, PDZD3, CX62, and UBN1) and synaptic function (ENAH, ITSN1, and SYT17). PARD3 is a well-known adaptor protein involved in asymmetrical cell division and in the formation of epithelial tight junctions through its interactions with other members of PARD family of proteins [40]. To test the reliability of the microarray gene expression fold changes, the expression of some of the genes (CDC42, EXOC4, PARD3, and PTP4A1) was confirmed by qRT-PCR, in additional cell

Table 1 Gene ontology enrichment analysis of differentially expressed genes using DAVID

Cluster	Enrichment score	Enriched term	Counts	PH	Benjamini
Upregulated genes					
1	1.8	Cell projection	20	697	2.0E−1
		Cell projection part	9	234	1.3E1
		Dendritic spine	4	38	1.5E1
		Neuron projection	10	342	3.5E1
		Dendrite	5	163	8.9E−1
2	1.37	Vacuolar membrane	4	56	3.7E1
		Vacuole	8	256	4.5E1
		Vacuole part	4	64	4.8E1
3	1.17	Cell junction	13	518	3.7E1
		Cell Junction	10	399	6.0E1
		Cell–Cell junction	5	190	9.7E1
		Synapse	5	213	9.9E1
Downregulated genes					
1	1.8	Positive regulation of cell migration	6	89	1.8E1
		Regulation of cell migration	8	169	9.9E1
		Positive regulation of cell motion	6	98	2.6E1
		Furin-like repeat	3	18	3.4E1
		Regulation of locomotion	8	192	3.9E1
		Basolateral plasma membrane	4	203	1.0E2

The counts and population hits (PH) are the number of genes in the gene list and background gene list, respectively, mapped to a specific term. Benjamini: p value after correcting for false discovery rate

lines treated with or without RT inhibition (Fig. 5b). We propose that the differences in gene expression in response to efavirenz described above are likely to be factors in the onset of cellular differentiation and morphological features seen in the drug-treated cells.

In the DAVID analysis of the list of downregulated genes, we found one statistically significant group (Table 1). This cluster contained a number of downregulated genes that are involved in the positive regulation of cell migration and movement (CHRD, PTENP1, PTP4A1, and TRIP6) and included a number of well-characterized oncogenes, epidermal growth factor receptor (v-erb-b

Fig. 5 RT inhibition modulates gene expression. **a** Heatmap of log2 expression values of genes in the four most significant gene annotation clusters identified by the DAVID analysis from lists of genes that were 2-fold up- or downregulated and with *p* value for differential expression ≤ 0.05 after Benjamini–Hochberg correction for multiple testing. The *color scale* corresponds to the degree of fold change. *Green* upregulated genes; *red* downregulated genes, *black* no change. **b** Confirmation of differentially expressed genes from the microarray expression profiling experiments. Relative levels of differentially expressed genes were quantified by qRT-PCR with primers specific for their sequences. The data are shown as the fold change compared to mock-treated cells after normalization to the HPRT1 housekeeping gene. Data are expressed as mean ± SD (*n* = 4)
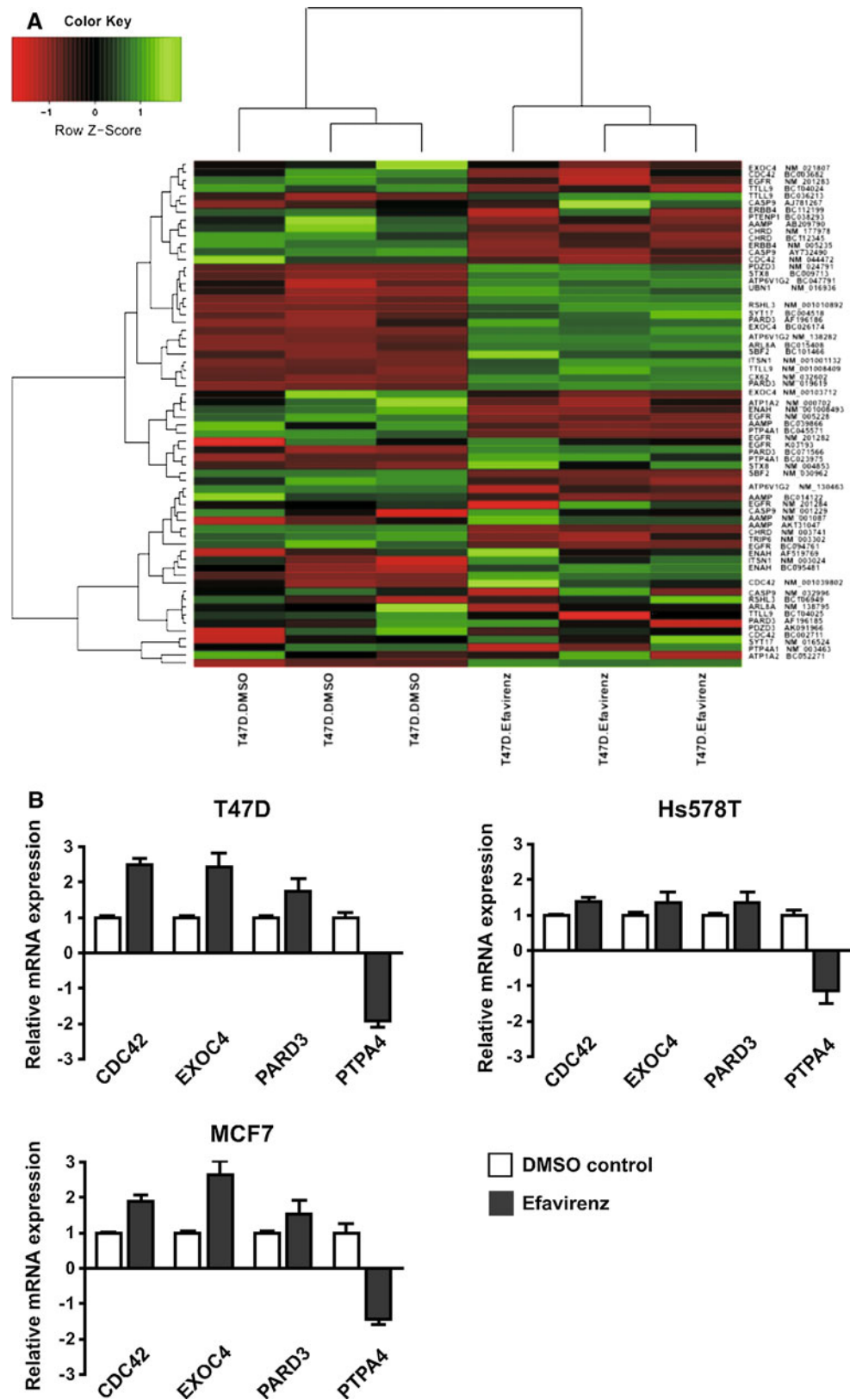
erythroblastic leukemia viral homolog) (EGFR) and the erythroblastic leukemia viral oncogene homolog (ERBB4). The most notable findings were of the downregulation of

PRL tyrosine phosphatase, PTP4A1 (which stimulates cell proliferation and invasive activity by downregulating p21 (Cip1/Waf1) protein [41]) and AAMP (which plays a role

in breast cancer cell migration [42]). qRT-PCR examination of the downregulation of PTP4A1 gene in additional cell lines confirmed close correlation with gene expression in the microarray experiment and the rate of proliferation and differentiation seen in those cells (Fig. 5b). In addition to the enriched annotation classes described above, the KEGG (Kyoto Encyclopedia of Genes and Genomes) pathways selected by DAVID as the most statistically significant suggested that a number of the downregulated genes, particularly tumor suppressor genes (PTENP1, CASP9) might potentially be involved in the p53 signaling pathway (data not shown). We also observed other less significant enrichment clusters, but many of these clusters contained only ankyrin repeat sequences whose biological significance is not yet clearly understood. Interestingly, several recent studies proposed that the activation of retrotransposons might influence the cell transcriptome by generating small regulatory RNAs or rewire transcriptional networks by providing the transposon-derived transcription factor binding sites (TBFs) for activation of many genes [43, 44]. Although, at present, it is not known how might L1 influence gene expression, our study demonstrates that the inhibition of L1-encoded RT modulates the expression of genes, many of which are involved in differentiation pathways and cell growth, and thus further studies are required in this direction. Nonetheless, the results presented here provide a direct functional link between the expression of L1 elements and the development of breast cancer. Looking at the induced genes that were specifically expressed in response to the drug treatment, it is clear that efavirenz triggers the expression of distinct set of genes that can functionally modulate growth and differentiation of cancer cells.

Discussion

The contribution of L1 retrotransposons to pathological processes other than those due to genomic insertions is poorly understood. The expression of L1 protein is significantly elevated in the most types of breast cancer cells [13, 24, 25], but the functional significance of this expression on gene regulation is unknown. In addition, it is unclear whether L1 expression is an active process that drives cancer growth or a secondary bystander of cancer transformation. Studies carried out in melanoma and prostate cancer cell lines have shown that efavirenz selectively inhibits endogenous RT activity without interfering with the telomerase-associated RT (TERT) enzyme [19, 31]. The inhibition of L1-encoded RT has been associated with reduced growth in cancer cells and in nude mice [8, 9, 18]. However, little is known about the molecular events that govern such cell growth and differentiation.

In the present study, we investigated the endogenous expression of the L1-encoded RT enzyme in a range of breast cancer cell lines and evaluated whether inhibition of RT induces morphological changes in these cells in a way that can be directly attributed to changes in gene expression. While there appears to be some differences in the level of RT expression, similar to the changes in the expression of L1 ORF2 protein seen in our recent study [13, 25], we observed that cell type-specific morphological differences in response to RT inhibition by efavirenz. T47D cells underwent the most marked changes in morphological differentiation with the appearance of filopodial projections protruding from the cell periphery, whereas MCF7 exhibited elongated microtubule extensions that adhered tightly to their substrate, similar to the phenotypic changes seen in melanoma A-375 and prostate cancer cell lines [18, 20]. Hs578T cells had a weak response to the drug. Concomitant with this, we also noticed reduced cell growth and proliferation which was largely independent of cell death or cytotoxicity. These observations suggest a causative role for L1-encoded RT in cancer growth. This is further supported by the finding that small interference RNAi against the L1-encoding RT enzyme induces morphological and proliferative changes that are almost identical to those caused by efavirenz and other NNRT1 drugs [18, 20]. Notably, however, downregulation of the HERV-encoded RT enzyme has no significant effects on cell proliferation and differentiation [19], suggesting that L1-encoded RT plays specific roles in pathological processes.

Given that efavirenz attenuates the tumorigenic phenotype of breast cancer cell lines, it is of obvious interest to determine the biological pathways affected by RT inhibition. Although it was previously shown that RT inhibition changes the expression of few cell cycle-related genes [18], a direct connection between the phenotypic changes induced by efavirenz and changes in gene expression has been largely missing. In this study we analyzed the global changes in gene expression that occur during RT inhibition. Using gene expression profiling with microarrays and GO enrichment analysis, our study identified three clusters of induced genes. The first upregulated cluster contained genes involved in cell projection and dendritic spine formation. This cluster included EXOC4 which is essential for the biogenesis of epithelial cell surfaces through its interactions with the actin cytoskeletal remodeling and vesicle transport machinery [45]. The cluster also contained CDC42 which regulates the signaling pathways that control the extension and maintenance of filopodia [33]. The second cluster contained genes involved in the cell cycle and genes associated with the centrosome and mitotic spindle formation. The third cluster contained genes involved in cell-to-cell junction formation (PARD3, PDZD3, CX62, and UBN1) and synaptic function (ENAH, ITSN1, and

SYT17). PARD3 is a member of a family of adaptor proteins playing a central role in the formation of epithelial tight junctions by interacting with other members of the PARD family of proteins [40]. Furthermore, the present study also identified a number of downregulated genes with roles in cell proliferation, cell migration and invasive activity, and that promote metastasis. Downregulation of PTP4A1 and AAMP are notable, and the expression of these genes is required for conferring transformed phenotypes in human cancers [41, 42], implicating their roles in the tumorigenesis. Strikingly, our study has identified that the downregulation of PTP4A1 is common in all RT-inhibited breast cancer cells. In summary, our study demonstrates that RT inhibition altered the expression of a number of key genes, which are functionally associated with cell projections, cell cycle progression, and cell-to-cell junctions. It appears possible that altered expression of these genes alone could be sufficient to revert undifferentiated cells to more differentiated phenotypes.

At this stage, the underlying mechanism of the activation or repression of gene expression that occurs during inhibition of RT is unclear. One possibility is that inhibition of RT substantially reduces the activity of L1 retrotransposition, which in turn reduces the restructuring of the genome and transcriptome that occurs during L1 retrotransposition [46]. One could therefore, argue that the changes in gene expression that follow RT inhibition and that were identified by our microarray analysis are likely to contribute to phenotypic changes. Another possibility is that L1-encoded RT may have a direct role in the transcriptional activation or repression of some of these genes. Recently, it has been postulated that the retrotransposition activity of L1 elements might interfere with the transcription machinery of cells and thereby be involved in the development and progression of cancer [47]. A computational study proposes that the expression of L1 elements may regulate the network of genes by contributing a source of transcriptional regulatory signals previously not present in the promoters of genes [48]. Remarkably, a recent study sequencing the 5′-most nucleotides of RNAs from normal, and neoplastic tissues identified that highly specific patterns of transcriptional activity occur due to the expression of L1 elements [49]. In addition, several other studies have reported that L1 elements in human cancer are capable of interfering with normal gene expression by providing alternative promoters for expression of nearby oncogenes [50] or by disrupting the expression of tumor suppressor genes by epigenetic dysregulation of L1 sequences [51]. Thus, it is possible that one or more of these mechanisms might contribute to the reduction in cell growth following inhibition of L1-encoded RT activity in breast cancer cells. Given that the observed phenotypic changes were reversible when RT inhibition was stopped, it is possible that RT inhibition may act through reversible epigenetic changes that alter the expression of genes. Consistent with this, there is growing evidence from studies with a number of drugs, which are currently in clinical trials [52], that epigenetic changes can bypass the genetic alterations caused by malignancy and reprogram gene expression by changing the epigenetic state of the cells. Thus, identifying the epigenetic mechanisms by which RT inhibition affects genome-wide gene expression may help us to understand the crosstalk between RT and the pathogenesis of breast cancer.

Conclusion

This study has explored the relationship between the expression of endogenous L1-encoded RT and the pathological features of breast cancer cells. In this study we have shown, first, that RT activity is widespread in breast cancer cells. Second, abnormal cell growth and the undifferentiated state of breast cancer cells are closely associated with RT activity. Inhibition of RT reduces cell proliferation (which is not related to cell death or cytotoxicity) and induces morphological differentiation of cancer cells. Third, RT inhibition modulates the expression of a distinct set of genes that are functionally associated with cell growth and differentiation. This study is the first to profile the changes in gene expression that occur during cell differentiation in relation to inhibition of L1-encoded RT by antiviral drugs. We found that considerable cell type-specific morphological differences exist in response to RT inhibition that may be related to the biological and pathological features of breast cancer cells. The association found between RT inhibition and the observed changes in gene expression suggest that further studies of the network of genes are warranted in breast cancer cells.

References

1. Belancio VP, Hedges DJ, Deininger P (2008) Mammalian non-LTR retrotransposons: for better or worse, in sickness and in health. Genome Res 18(3):343–358. doi:10.1101/gr.5558208

2. Cordaux R, Batzer MA (2009) The impact of retrotransposons on human genome evolution. Nat Rev Genet 10(10):691–703. doi:10.1038/nrg2640

3. Brouha B, Schustak J, Badge RM, Lutz-Prigge S, Farley AH, Moran JV, Kazazian HH Jr (2003) Hot L1s account for the bulk of retrotransposition in the human population. Proc Natl Acad Sci USA 100(9):5280–5285

4. Beck CR, Collier P, Macfarlane C, Malig M, Kidd JM, Eichler EE, Badge RM, Moran JV (2010) LINE-1 retrotransposition activity in human genomes. Cell 141(7):1159–1170. doi:10.1016/j.cell.2010.05.021

5. Dewannieux M, Esnault C, Heidmann T (2003) LINE-mediated retrotransposition of marked Alu sequences. Nat Genet 35(1):41–48. doi:10.1038/ng1223

6. Garcia-Perez JL, Doucet AJ, Bucheton A, Moran JV, Gilbert N (2007) Distinct mechanisms for trans-mediated mobilization of cellular RNAs by the LINE-1 reverse transcriptase. Genome Res 17(5):602–611. doi:10.1101/gr.5870107

7. Kazazian HH Jr (2004) Mobile elements: drivers of genome evolution. Science 303(5664):1626–1632. doi:10.1126/science.1089670

8. Sinibaldi-Vallebona P, Lavia P, Garaci E, Spadafora C (2006) A role for endogenous reverse transcriptase in tumorigenesis and as a target in differentiating cancer therapy. Genes Chromosom Cancer 45(1):1–10. doi:10.1002/gcc.20266

9. Sciamanna I, Vitullo P, Curatolo A, Spadafora C (2009) Retrotransposons, reverse transcriptase and the genesis of new genetic information. Gene 448(2):180–186. doi:10.1016/j.gene.2009.07.011

10. Spadafora C (2004) Endogenous reverse transcriptase: a mediator of cell proliferation and differentiation. Cytogenet Genome Res 105(2–4):346–350. doi:10.1159/000078207

11. Asch HL, Eliacin E, Fanning TG, Connolly JL, Bratthauer G, Asch BB (1996) Comparative expression of the LINE-1 p40 protein in human breast carcinomas and normal breast tissues. Oncol Res 8(6):239–247

12. Belancio VP, Roy-Engel AM, Deininger PL (2010) All y'all need to know 'bout retroelements in cancer. Semin Cancer Biol 20(4):200–210. doi:10.1016/j.semcancer.2010.06.001

13. Chen L, Dahlstrom JE, Lee SH, Rangasamy D (2012) Naturally occurring endo-siRNA silences LINE-1 retrotransposons in human cells through DNA methylation. Epigenetics 7(7):758–771. doi:10.4161/epi.20706

14. Golan M, Hizi A, Resau JH, Yaal-Hahoshen N, Reichman H, Keydar I, Tsarfaty I (2008) Human endogenous retrovirus (HERV-K) reverse transcriptase as a breast cancer prognostic marker. Neoplasia 10(6):521–533

15. Contreras-Galindo R, Kaplan MH, Leissner P, Verjat T, Ferlenghi I, Bagnoli F, Giusti F, Dosik MH, Hayes DF, Gitlin SD, Markovitz DM (2008) Human endogenous retrovirus K (HML-2) elements in the plasma of people with lymphoma and breast cancer. J Virol 82(19):9329–9336. doi:10.1128/JVI.00646-08

16. Kurth R, Bannert N (2010) Beneficial and detrimental effects of human endogenous retroviruses. Int J Cancer 126(2):306–314. doi:10.1002/ijc.24902

17. De Clercq E (1993) HIV-1-specific RT inhibitors: highly selective inhibitors of human immunodeficiency virus type 1 that are specifically targeted at the viral reverse transcriptase. Med Res Rev 13(3):229–258

18. Sciamanna I, Landriscina M, Pittoggi C, Quirino M, Mearelli C, Beraldi R, Mattei E, Serafino A, Cassano A, Sinibaldi-Vallebona P, Garaci E, Barone C, Spadafora C (2005) Inhibition of endogenous reverse transcriptase antagonizes human tumor growth. Oncogene 24(24):3923–3931. doi:10.1038/sj.onc.1208562

19. Oricchio E, Sciamanna I, Beraldi R, Tolstonog GV, Schumann GG, Spadafora C (2007) Distinct roles for LINE-1 and HERV-K retroelements in cell proliferation, differentiation and tumor progression. Oncogene 26(29):4226–4233. doi:10.1038/sj.onc.1210214

20. Sbardella G, Bartolini S, Castellano S, Artico M, Paesano N, Rotili D, Spadafora C, Mai A (2006) 6-alkylthio-4-[1-(2,6-difluorophenyl)alkyl]-1H-[1,3,5]triazin-2-ones (ADATs): novel regulators of cell differentiation and proliferation. ChemMedChem 1(10):1073–1080. doi:10.1002/cmdc.200600139

21. Jones RB, Garrison KE, Wong JC, Duan EH, Nixon DF, Ostrowski MA (2008) Nucleoside analogue reverse transcriptase inhibitors differentially inhibit human LINE-1 retrotransposition. PLoS ONE 3(2):e1547. doi:10.1371/journal.pone.0001547

22. Dai L, Huang Q, Boeke JD (2011) Effect of reverse transcriptase inhibitors on LINE-1 and Ty1 reverse transcriptase activities and on LINE-1 retrotransposition. BMC Biochem 12:18. doi:10.1186/1471-2091-12-18

23. Carlini F, Ridolfi B, Molinari A, Parisi C, Bozzuto G, Toccacieli L, Formisano G, De Orsi D, Paradisi S, Grober OM, Ravo M, Weisz A, Arcieri R, Vella S, Gaudi S (2010) The reverse transcription inhibitor abacavir shows anticancer activity in prostate cancer cell lines. PLoS ONE 5(12):e14221. doi:10.1371/journal.pone.0014221

24. Harris CR, Normart R, Yang Q, Stevenson E, Haffty BG, Ganesan S, Cordon-Cardo C, Levine AJ, Tang LH (2010) Association of nuclear localization of a long interspersed nuclear element-1 protein in breast tumors with poor prognostic outcomes. Genes Cancer 1(2):115–124. doi:10.1177/1947601909360812

25. Chen L, Dahlstrom JE, Chandra A, Board P, Rangasamy D (2012) Prognostic value of LINE-1 retrotransposon expression and its subcellular localization in breast cancer. Breast Cancer Res Treat 136(1):129–142. doi:10.1007/s10549-012-2246-7

26. van Hoesel AQ, van de Velde CJ, Kuppen PJ, Liefers GJ, Putter H, Sato Y, Elashoff DA, Turner RR, Shamonki JM, de Kruijf EM, van Nes JG, Giuliano AE, Hoon DS (2012) Hypomethylation of LINE-1 in primary tumor has poor prognosis in young breast cancer patients: a retrospective cohort study. Breast Cancer Res Treat 134(3):1103–1114. doi:10.1007/s10549-012-2038-0

27. Merluzzi VJ, Hargrave KD, Labadia M, Grozinger K, Skoog M, Wu JC, Shih CK, Eckner K, Hattox S, Adams J et al (1990) Inhibition of HIV-1 replication by a nonnucleoside reverse transcriptase inhibitor. Science 250(4986):1411–1413

28. Timpl R, Dziadek M (1986) Structure, development, and molecular pathology of basement membranes. Int Rev Exp Pathol 29:1–112

29. Liotta LA, Rao CN, Wewer UM (1986) Biochemical interactions of tumor cells with the basement membrane. Annu Rev Biochem 55:1037–1057. doi:10.1146/annurev.bi.55.070186.005133

30. Daneker GW Jr, Piazza AJ, Steele GD Jr, Mercurio AM (1989) Relationship between extracellular matrix interactions and degree of differentiation in human colon carcinoma cell lines. Cancer Res 49(3):681–686

31. Mangiacasale R, Pittoggi C, Sciamanna I, Careddu A, Mattei E, Lorenzini R, Travaglini L, Landriscina M, Barone C, Nervi C, Lavia P, Spadafora C (2003) Exposure of normal and transformed cells to nevirapine, a reverse transcriptase inhibitor, reduces cell growth and promotes differentiation. Oncogene 22(18):2750–2761. doi:10.1038/sj.onc.1206354

32. Small JV, Geiger B, Kaverina I, Bershadsky A (2002) How do microtubules guide migrating cells? Nat Rev Mol Cell Biol 3(12):957–964. doi:10.1038/nrm971

33. Mattila PK, Lappalainen P (2008) Filopodia: molecular architecture and cellular functions. Nat Rev Mol Cell Biol 9(6):446–454. doi:10.1038/nrm2406

34. Lange K (2011) Fundamental role of microvilli in the main functions of differentiated cells: outline of an universal regulating and signaling system at the cell periphery. J Cell Physiol 226(4):896–927. doi:10.1002/jcp.22302

35. Snapper SB, Takeshima F, Anton I, Liu CH, Thomas SM, Nguyen D, Dudley D, Fraser H, Purich D, Lopez-Ilasaca M, Klein C, Davidson L, Bronson R, Mulligan RC, Southwick F, Geha R, Goldberg MB, Rosen FS, Hartwig JH, Alt FW (2001) N-WASP deficiency reveals distinct pathways for cell surface projections and microbial actin-based motility. Nat Cell Biol 3(10):897–904. doi:10.1038/ncb1001-897

36. Lange K (2002) Role of microvillar cell surfaces in the regulation of glucose uptake and organization of energy metabolism. Am J Physiol Cell Physiol 282(1):C1–C26

37. McClay DR (1999) The role of thin filopodia in motility and morphogenesis. Exp Cell Res 253(2):296–301. doi:10.1006/excr.1999.4723

38. Schober JM, Komarova YA, Chaga OY, Akhmanova A, Borisy GG (2007) Microtubule-targeting-dependent reorganization of filopodia. J Cell Sci 120(Pt 7):1235–1244. doi:10.1242/jcs.003913

39. Nilufar S, Morrow AA, Lee JM, Perkins TJ (2013) FiloDetect: automatic detection of filopodia from fluorescence microscopy images. BMC Syst Biol 7:66. doi:10.1186/1752-0509-7-66

40. Tepass U, Tanentzapf G, Ward R, Fehon R (2001) Epithelial cell polarity and cell junctions in Drosophila. Annu Rev Genet 35:747–784. doi:10.1146/annurev.genet.35.102401.091415

41. Werner SR, Lee PA, DeCamp MW, Crowell DN, Randall SK, Crowell PL (2003) Enhanced cell cycle progression and down regulation of p21(Cip1/Waf1) by PRL tyrosine phosphatases. Cancer Lett 202(2):201–211

42. Yin Y, Sanders AJ, Jiang WG (2013) The impact of angio-associated migratory cell protein (AAMP) on breast cancer cells in vitro and its clinical significance. Anticancer Res 33(4):1499–1509

43. Kapusta A, Kronenberg Z, Lynch VJ, Zhuo X, Ramsay L, Bourque G, Yandell M, Feschotte C (2013) Transposable elements are major contributors to the origin, diversification, and regulation of vertebrate long noncoding RNAs. PLoS Genet 9(4):e1003470. doi:10.1371/journal.pgen.1003470

44. Kunarso G, Chia NY, Jeyakani J, Hwang C, Lu X, Chan YS, Ng HH, Bourque G (2010) Transposable elements have rewired the core regulatory network of human embryonic stem cells. Nat Genet 42(7):631–634. doi:10.1038/ng.600

45. Grindstaff KK, Yeaman C, Anandasabapathy N, Hsu SC, Rodriguez-Boulan E, Scheller RH, Nelson WJ (1998) Sec6/8 complex is recruited to cell–cell contacts and specifies transport vesicle delivery to the basal-lateral membrane in epithelial cells. Cell 93(5):731–740

46. Huang CR, Schneider AM, Lu Y, Niranjan T, Shen P, Robinson MA, Steranka JP, Valle D, Civin CI, Wang T, Wheelan SJ, Ji H, Boeke JD, Burns KH (2010) Mobile interspersed repeats are major structural variants in the human genome. Cell 141(7):1171–1182. doi:10.1016/j.cell.2010.05.026

47. Han JS, Boeke JD (2005) LINE-1 retrotransposons: modulators of quantity and quality of mammalian gene expression? BioEssays 27(8):775–784. doi:10.1002/bies.20257

48. Ramos KS, He Q, Kalbfleisch T, Montoya-Durango DE, Teneng I, Stribinskis V, Brun M (2007) Computational and biological inference of gene regulatory networks of the LINE-1 retrotransposon. Genomics 90(2):176–185. doi:10.1016/j.ygeno.2007.04.003

49. Iskow RC, McCabe MT, Mills RE, Torene S, Pittard WS, Neuwald AF, Van Meir EG, Vertino PM, Devine SE (2010) Natural mutagenesis of human genomes by endogenous retrotransposons. Cell 141(7):1253–1261. doi:10.1016/j.cell.2010.05.020

50. Wolff EM, Byun HM, Han HF, Sharma S, Nichols PW, Siegmund KD, Yang AS, Jones PA, Liang G (2010) Hypomethylation of a LINE-1 promoter activates an alternate transcript of the MET oncogene in bladders with cancer. PLoS Genet 6(4):e1000917

51. Shukla R, Upton KR, Munoz-Lopez M, Gerhardt DJ, Fisher ME, Nguyen T, Brennan PM, Baillie JK, Collino A, Ghisletti S, Sinha S, Iannelli F, Radaelli E, Dos Santos A, Rapoud D, Guettier C, Samuel D, Natoli G, Carninci P, Ciccarelli FD, Garcia-Perez JL, Faivre J, Faulkner GJ (2013) Endogenous retrotransposition activates oncogenic pathways in hepatocellular carcinoma. Cell 153(1):101–111. doi:10.1016/j.cell.2013.02.032

52. Nebbioso A, Carafa V, Benedetti R, Altucci L (2012) Trials with 'epigenetic' drugs: an update. Mol Oncol 6(6):657–682. doi:10.1016/j.molonc.2012.09.004